

**Best Available  
Copy  
for all Pictures**

AD-A011 925

EXCIMER LASERS

A. J. Palmer

Hughes Research Laboratories

Prepared for:

Defense Advanced Research Projects Agency  
Office of Naval Research

June 1975

DISTRIBUTED BY:

**NTIS**

National Technical Information Service  
U. S. DEPARTMENT OF COMMERCE

198023

11

ADA011925

# EXCIMER LASERS

A. J. PALMER

HUGHES RESEARCH LABORATORIES  
3011 MALIBU CANYON ROAD  
MALIBU, CA 90265

JUNE 1975

CONTRACT N00014-75-C-0081  
SEMIANNUAL TECHNICAL REPORT  
FOR PERIOD 1 OCTOBER 1974 THROUGH 31 MARCH 1975

DDC  
RECEIVED  
JUN 19 1975  
RECEIVED  
B

SPONSORED BY  
DEFENSE ADVANCED RESEARCH PROJECTS AGENCY  
DARPA ORDER NO. 1807

MONITORED BY  
OFFICE OF NAVAL RESEARCH

DISTRIBUTION STATEMENT A  
Approved for public release  
Distribution Unlimited

Reproduced by  
NATIONAL TECHNICAL  
INFORMATION SERVICE  
U.S. Department of Commerce  
Springfield, VA. 22151

DARPA Order No.	1807
Program Code No.	5E20
Contractor	Hughes Research Laboratories
Effective Date of Contract	1 October 1974
Contract Expiration Date	15 August 1975
Amount of Contract	\$99,000.00
Contract No.	N00014-75-C-0081
Principal Investigator	A. Jay Palmer
Phone No.	(213) 456-6411, extension 356
Title of Work	Excimer Lasers

ACCESSION for	
NTIS	White Section <input checked="" type="checkbox"/>
DTC	Blue Section <input type="checkbox"/>
UNCLASSIFIED	<input type="checkbox"/>
JUSTIFICATION	
BY	
DISTRIBUTION/AVAILABILITY CODES	
Dist.	AVAIL. and/or SPECIAL
A	

The views and conclusions contained in this document are those of the authors and should not be interpreted as necessarily representing the official policies, either expressed or implied, of the Defense Advanced Research Projects Agency or the U. S. Government.

UNCLASSIFIED

SECURITY CLASSIFICATION OF THIS PAGE (When Data Entered)

REPORT DOCUMENTATION PAGE		READ INSTRUCTIONS BEFORE COMPLETING FORM
1. REPORT NUMBER	2. GOVT ACCESSION NO.	3. RECIPIENT'S CATALOG NUMBER
4. TITLE (and Subtitle)  EXCIMER LASERS		5. TYPE OF REPORT & PERIOD COVERED Semiannual Tech. Rpt. 1 Oct 1974-31 March 1975
		6. PERFORMING ORG. REPORT NUMBER
7. AUTHOR(s)  A. J. Palmer		8. CONTRACT OR GRANT NUMBER(s)  N00014-75-C-0031
9. PERFORMING ORGANIZATION NAME AND ADDRESS Hughes Research Laboratories 3011 Malibu Canyon Road Malibu, CA 90265		10. PROGRAM ELEMENT PROJECT, TASK AREA & WORK UNIT NUMBERS Arpa Order No. 1807 Program Code No. 5E20
11. CONTROLLING OFFICE NAME AND ADDRESS Defense Advanced Research Projects Agency Arlington, VA 22209		12. REPORT DATE June 1975
		13. NUMBER OF PAGES 41
14. MONITORING AGENCY NAME & ADDRESS (if different from Controlling Office) Office of Naval Research 800 N. Quincy Street Arlington, VA 22217		15. SECURITY CLASS. (of this report) Unclassified
		15a. DECLASSIFICATION DOWNGRADING SCHEDULE
16. DISTRIBUTION STATEMENT (of this Report)		
17. DISTRIBUTION STATEMENT (of the abstract entered in Block 20, if different from Report)		
18. SUPPLEMENTARY NOTES		
19. KEY WORDS (Continue on reverse side if necessary and identify by block number) Excimer Lasers, Dimer Lasers, Alkali-Rare Gas Lasers, Continuum Lasers		
20. ABSTRACT (Continue on reverse side if necessary and identify by block number) The general goals of this program are to identify the required operating conditions for achieving practical net laser gain for an alkali-rare gas laser transition for optical pumping, avalanche discharge pumping and ultraviolet-sustainer discharge pumping, and to demonstrate net laser gain in the laboratory with one of the three pumping techniques. Substantial progress has already been made		

D D C  
RECEIVED  
JUN 19 1975  
RECEIVED  
B

UNCLASSIFIED

SECURITY CLASSIFICATION OF THIS PAGE (When Data Entered)

toward achieving these goals and by the end of the current program we anticipate complete realization of these goals.

A versatile computer code which contains all relevant gas-kinetic processes, optical pumping processes, and electronic plasma processes has been developed and computes small-signal gain and absorption coefficients versus wavelength due to both alkali-rare gas molecules and alkali dimer molecules. The code is currently operational and is being used at present to guide the discharge and optical pumping experimental studies of the potassium-xenon system. The code predicts net laser gain for this system under readily available operating conditions using optical pumping, and under operating conditions which may be available (depending on discharge stability) for discharge pumping.

Optical absorption measurements on the K-Xe system have been carried out clearly showing the contribution from both ground state K-Xe molecules and  $K_2$  molecules, with a wavelength profile in agreement with that predicted by the model. Fluorescence measurements on the discharge experiment have also been carried out showing both the excimer and dimer states in emission.

Currently, attempts are being made to both measure the gain directly using a GaAs probe laser and to achieve laser oscillation on the flashlamp-pumped K-Xe system. Preliminary data have been obtained with the probe laser technique which may indicate gain but are inconclusive at present pending the elimination of a fluctuation problem.

UNCLASSIFIED

SECURITY CLASSIFICATION OF THIS PAGE (When Data Entered)

## TABLE OF CONTENTS

Section		Page
I	INTRODUCTION . . . . .	7
II	THEORETICAL PROGRAM . . . . .	9
	A. Optical Pumping . . . . .	10
	B. Discharge Pumping . . . . .	14
III	EXPERIMENTAL PROGRAM . . . . .	25
	A. Discharge Experiments . . . . .	25
	B. Flashlamp Pumping Experiments . . . . .	33
IV	FUTURE PROGRAM PLAN . . . . .	41
	A. Theoretical Modeling . . . . .	41
	B. Experimental Program . . . . .	41
	C. Alkali Source Studies . . . . .	41
	REFERENCES . . . . .	43

## LIST OF ILLUSTRATIONS

Figure		Page
II-1	Potassium-Xenon Energy Flow Diagram – Optical Pumping . . . . .	12
II-2	Potassium-Xenon Theoretical, Small-Signal Laser Gain – Optical Pumping . . . . .	15
II-3	Potassium-Xenon Energy Flow Diagram – Discharge Pumping . . . . .	16
II-4	Potassium-Xenon Theoretical, Small-Signal Laser Gain – Self-Sustained Discharge . . . . .	21
II-5	Potassium-Xenon Theoretical, Small-Signal Laser Gain – Ultraviolet-Sustained Discharge . . . . .	22
III-1	Experimental Apparatus – Flashlamp Pumping . . . . .	26
III-2	Experimental Apparatus – Discharge Pumping . . . . .	26
III-3	Potassium-Xenon Absorption Coefficient: Comparison of Measurements to Theoretical Model (Low Temperature Results) . . . . .	27
III-4	Potassium-Xenon Absorption Coefficient: Comparison of Measurements to Theoretical Model (High Temperature Results) . . . . .	28
III-5	Present Transverse Discharge Design . . . . .	29
III-6	Current and Excimer Fluorescence Waveforms . . . . .	30
III-7	Excimer Emission Spectral Profiles . . . . .	32
III-8	Potassium-Argon Discharge Fluorescence Comparison of Measurements with Theoretical Model . . . . .	34
III-9	Current Experimental Apparatus . . . . .	35
III-10	Photograph of Current Apparatus . . . . .	36
III-11	Probe Laser Gain Measurement Technique . . . . .	39
III-12	Flashlamp Output Measurements . . . . .	40

## I. INTRODUCTION

The A to X transition on the diatomic alkali rare gas molecules (excimers) and the diatomic alkali molecules (dimers) are now well recognized as a potentially efficient, high average power, tunable laser transition.<sup>1,2</sup> At a rare gas pressure of ~10 atm and an alkali partial pressure of a fraction of a Torr, both the excimer and dimer transitions can exhibit practical laser gain for pumping by flashlamps, discharges, or electron beams. At these pressures both the dimer transitions (for the heavier alkalis) as well as the excimer transitions are continuum transitions, each roughly a thousand angstroms wide, and lie in the near infrared to visible portion of the spectrum.

The primary goals of the present program are to identify specific operating conditions for achieving laser oscillation on the dimer and excimer transitions of all of the alkali xenon systems and to demonstrate net laser gain in a laboratory apparatus from at least one of these systems. These goals are well on the way to completion.

A versatile computer code, which contains all relevant gas-kinetic processes and plasma processes, has been developed for optical pumping, avalanche discharge pumping, and ultraviolet sustainer discharge pumping, and computes small-signal gain and absorption coefficients versus wavelength due to both alkali-rare gas molecules and alkali dimer molecules. The code is currently operational and is being used at present to guide the discharge and optical pumping experimental studies of the potassium-xenon (K-Xe) system. The code predicts net laser gain for this system under operating conditions being realized in the laboratory for optical pumping and under operating conditions which may be available, depending on discharge stability, for discharge pumping.

In the measurements phase of the program, optical absorption measurements on the K-Xe system have been carried out, clearly showing the contribution from both ground state K-Xe molecules and K<sub>2</sub> molecules, with a wavelength profile in agreement with that

predicted by the model. Fluorescence measurements on the discharge experiment have also been carried out showing both the excimer and dimer states in emission. Experiments are currently under way to measure the gain on the K-Xe excimer band directly through the use of a GaAs 8215 Å probe laser. A review of the experimental program will be presented in Section III.

The anticipated work plan for the remainder of the current program will be discussed in Section IV.

## II. THEORETICAL PROGRAM

The first step in the theoretical program is to calculate, from the shape of the potential energy curves, the stimulated emission and absorption coefficients as a function of wavelength for the excimer and dimer transitions involved. Except for lithium, the wavelength range of all of the alkali dimer A-X transitions will overlap that of the associated alkali-rare gas excimer transition. It is essential, therefore, that the dimer transition be included in the calculation of the net absorption, especially since the dimer concentration will increase more rapidly with an increase in alkali concentration than will the excimer molecules, thereby eventually dominating the absorption. The alkali-dimer transition can also have a net gain, so the dimer stimulated emission coefficient is computed as well.

The stimulated emission and absorption coefficients are computed using the quasi-static theory of line broadening.<sup>3</sup> This theory assumes that individual vibrational transitions have been broadened into a continuum and that the molecular electronic state is populated through a continuum of internuclear separations according to a classical canonical energy distribution. The stimulated emission and absorption coefficient, for the A to X transition, can then be written as

$$g(\nu) = [A] \frac{A(\nu)c^2 4\pi R^2}{8\pi\nu^2 d\nu/dR} \exp \left[ -\frac{\frac{V_A(R)}{kT} \frac{g}{g_{fA}}}{\left( K_A \frac{g_{fA}}{g_A} \right)} \right] \quad (1)$$

$$\beta(\nu) = [X] \frac{A(\nu)c^2 4\pi R^2}{8\pi\nu^2 d\nu/dR} \left( \frac{g_A}{g_X} \right) \exp \left[ -\frac{\frac{V_X(R)}{kT} \frac{g}{g_{fX}}}{\left( K_X \frac{g_{fX}}{g_X} \right)} \right] \quad (2)$$

Here,  $[A]$  and  $[X]$  are the molecular A state and X state concentrations, and  $g_A, g_X, g_{fA}, g_{fX}$  are the degeneracy factors for the A and X states and their parent atomic states, respectively.  $A(\nu)$  is the Einstein A coefficient for the transition (possibly dependent on internuclear separation),  $R$  is the internuclear separation,  $\nu$  is the frequency of the transition,  $V_A(R)$  and  $V_X(R)$  are the potential energies of the A state and X state measured relative to their parent atomic states,  $K_A$  and  $K_X$  are equilibrium constants for the A and X states,  $T_g$  is the gas temperature, and  $c$  is the speed of light.

Note that these expressions do not necessarily assume thermal equilibrium to be present between molecular states and their parent atomic states. A full rate equation analysis is employed to calculate the A state and the parent atomic state concentrations. Such calculations have been performed for optical pumping, discharge pumping, and ultraviolet sustainer discharge pumping and are described in detail below.

#### A. Optical Pumping

The optical pumping concept employed in the current study involves the use of a broad band source, such as a xenon flashlamp, to pump into the absorption bands of the excimer and dimer transitions themselves. Thus the primary pumping rate,  $R$ , is computed by simply integrating over the transition bandwidth, the product of incident flashlamp spectral flux times the net absorption coefficient (including stimulated emission) times a factor which accounts for the penetration depth of the flashlamp flux into the mixture.

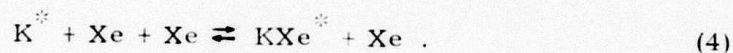
$$R_{E,D} = \int \phi(\nu) \beta_{E,D}(\nu) \exp \{ -[\beta_E(\nu) + \beta_D(\nu)]x \} d\nu, \quad (3)$$

where  $\phi(\nu)$  is the pump spectral intensity in photons per square centimeter per frequency interval,  $\beta_{E,D}$  is the absorption coefficient for the excimer or dimer, and  $x$  is the propagation distance of the pump radiation into the mixture. This pumping rate for both dimers and

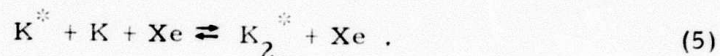
excimers are then entered into three coupled rate equations governing the population of the excimer upper laser level, the dimer upper laser level, and the alkali resonance level. The ground state species are assumed to remain in thermal equilibrium with one another and the alkali vapor pressure is assumed in equilibrium with its condensate at the gas temperature.

The following formation and destruction processes for the excited states are included in the rate equation analysis (using nomenclature for the K-Xe system):

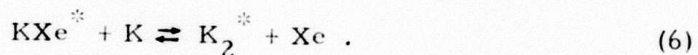
Excimer dissociation and association:



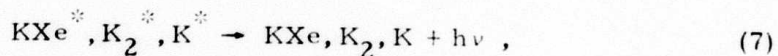
Dimer dissociation and association:



Excimer-dimer exchange reactions:



Radiative decay:



where the  $K^*$  decay is governed by radiation trapping. An energy flow diagram showing the potassium excimer and dimer potential energy curves is presented in Fig. II-1. The excimer potential curves are obtained from Ref. 4 and the dimer curves are from Ref. 2.

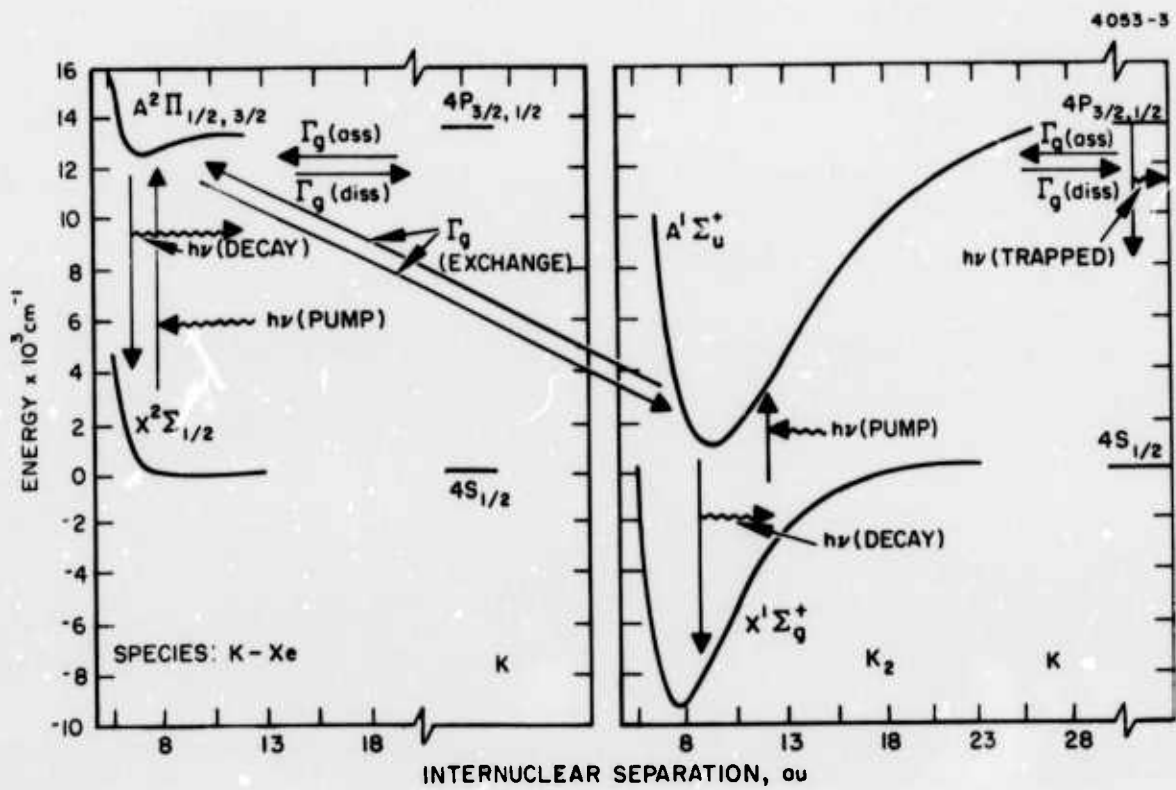


Fig. II-1. Potassium-xenon energy flow diagram - optical pumping.

The rate equations for these reactions are written as follows:

Excimer level rate equation:

$$\begin{aligned} \frac{d}{dt} [KXe^*] &= R_E + \Gamma_{\text{ass}(E)}[K^*] + \Gamma_{\text{ex}}[K_2^*] \\ &- (\Gamma_{\text{ex}}' + \Gamma_{\text{diss}(E)} + A + S_E)[KXe^*] = 0 . \end{aligned} \quad (8)$$

Dimer level rate equation:

$$\begin{aligned} \frac{d}{dt} [K_2^*] &= R_D + \Gamma_{\text{ass}(D)}[K^*] + \Gamma_{\text{ex}}'[KXe^*] \\ &- (\Gamma_{\text{ex}} + \Gamma_{\text{diss}(D)} + A + S_D)[K_2^*] = 0 . \end{aligned} \quad (9)$$

Resonance level rate equation:

$$\begin{aligned} \frac{d}{dt} [K^*] &= \Gamma_{\text{diss}(E)}[KXe^*] + \Gamma_{\text{diss}(D)}[K_2^*] \\ &- (\Gamma_{\text{ass}(E)} + \Gamma_{\text{ass}(D)} + A_{\text{tr}})[K^*] = 0 , \end{aligned} \quad (10)$$

where  $\Gamma_{\text{ass}}$  and  $\Gamma_{\text{diss}}$  are the association and dissociation rates for reactions (4)(E) and (5)(D),  $\Gamma_{\text{ex}}$  and  $\Gamma_{\text{ex}}'$  are the forward and backward excimer-dimer exchange reaction rates for reaction (6),  $A$  is the excimer and dimer level radiative rate,  $A_{\text{tr}}$  is the trapped radiative rate for the resonance level, and  $S_E$  and  $S_D$  are stimulated A to X transition rates induced by the pump field. The transition rates  $S_E$  and  $S_D$  are given by expressions analogous to eq. (3):

$$S_{E,D} = \int \phi(\nu)(g_{E,D}(\nu)/[A]) \exp[-\beta_E(\nu) + \beta_D(\nu)x] d\nu .$$

The forward and backward rates for reactions (3) through (5) are related by detailed balancing and Saha's equation:

$$\Gamma_{\text{ass, E, D}} / \Gamma_{\text{diss, E, D}} = [\text{Xe}] K_{A_{E, D}}$$

$$\Gamma_{\text{ex}}^{\text{D}} / \Gamma_{\text{ex}}^{\text{E}} = \frac{[\text{Xe}]}{[\text{K}]} \cdot \frac{K_{A_{E}}}{K_{A_{D}}}$$

The values for the association rate is obtained from the literature or through scaling arguments applied to measured rates for other systems following Ref. (2).

Table II-1 lists the numerical values of the rates used in eqs. (8) through (10) for the K-Xe system.

A computer code has been set up which solves eqs. (1), (2), and the rate equations and calculates absorption and net gain for input values of gas temperature, xenon concentrations, and incident flashlamp flux. Sample results for the K-Xe system with a flashlamp flux chosen to be consistent with measured xenon flashlamp outputs are shown in Fig. II-2. One can see that practical laser gain is predicted from both the excimer and dimer at temperatures and pressures readily achievable in a laboratory experiment. Note that at the higher temperature the gain shifts to the dimer band as anticipated.

#### B. Discharge Pumping

A computer model analogous to that for optical pumping has also been developed for discharge pumping. The laser kinetics modeling is the same as before, except that excitation and de-excitation of the electronic states occur via inelastic and superelastic electron collisions, as illustrated in Fig. II-3. In this case, under typical operating conditions most of the pumping occurs through the excitation of the atomic resonance level.

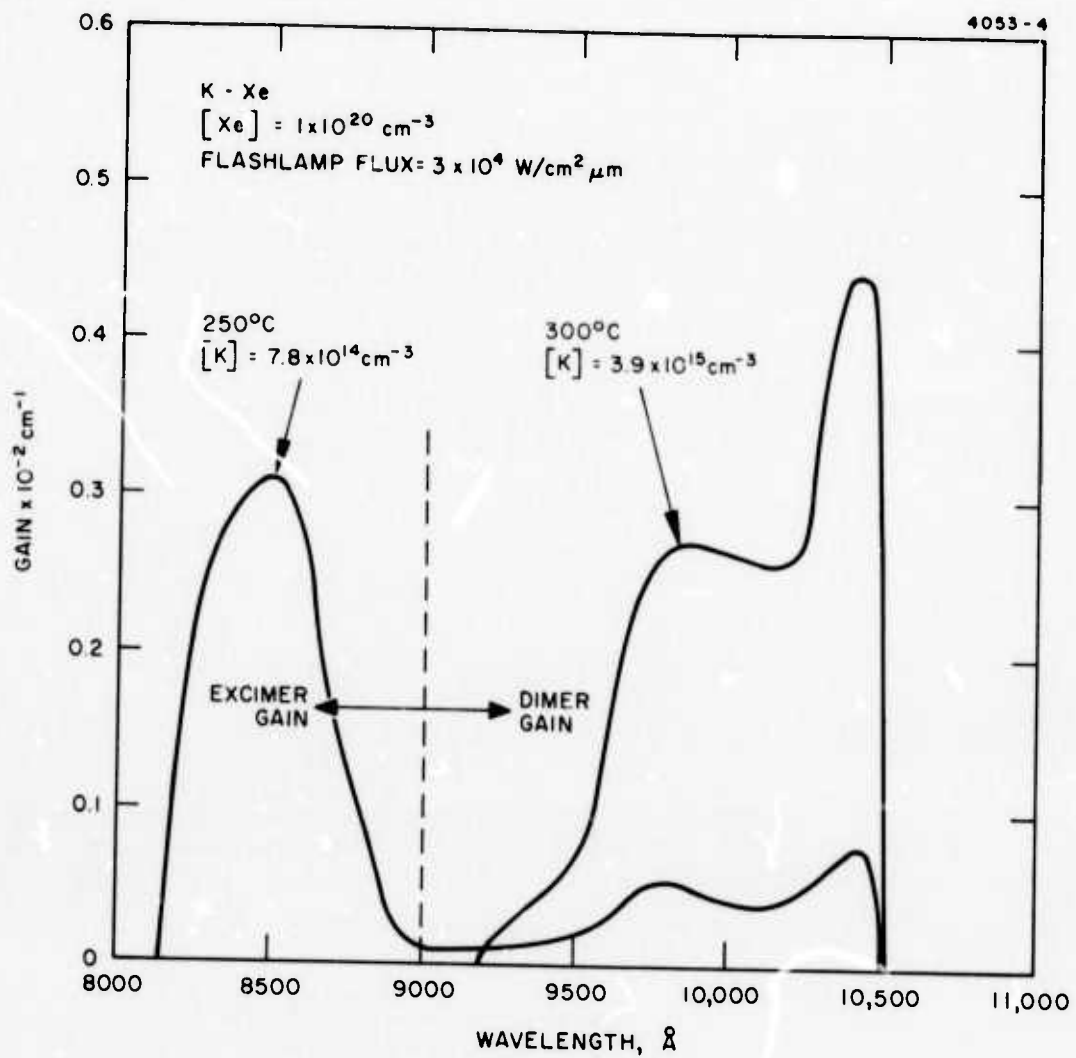


Fig. II-2. Potassium-xenon theoretical, small-signal laser gain - optical pumping.



Table II-1  
RATE CONSTANTS USED IN OPTICAL  
PUMPING MODEL

Rate	Numerical Value	Reference
A	$3.69 \times 10^7 \text{ sec}$	6
$K_{A_E}$	$2.2 \times 10^{-23} \exp\left(\frac{0.074}{T_g}\right) \text{ cm}^3$	2
$K_{A_D}$	$6.9 \times 10^{-21} \exp\left(\frac{0.496}{T_g}\right) \text{ cm}^3$	2
$\Gamma_{\text{ass}_E}$	$8.2 \times 10^{-32} \times [\text{Xe}]^2 \text{ sec}^{-1}$	2
$\Gamma_{\text{ass}_D}$	$8.0 \times 10^{-30} \times [\text{Xe}] \times [\text{K}] \text{ sec}^{-1}$	2
$\Gamma_{\text{ex}}'$	$1 \times 10^{-10} \times [\text{K}] \text{ sec}^{-1}$	Estimate

T1665

A plasma model is also incorporated into the computer code which computes the electron density and electron temperature to be used in the kinetics model.

An outline of the plasma model in its current state is presented below (again using the notation for the K-Xe system).

1. Electron Energy Distribution

A maxwellian energy distribution for the electrons is assumed. This assumption is not expected to lead to serious error since most of the excitation processes of concern to us will involve electrons with near average energy rather than those on the tail of the distribution where large departures from maxwellian population can occur.

## 2. Electron Temperature

Electrons are assumed to gain energy from the field and lose energy in steady state through elastic collisions with the rare gas and inelastic collisions with the alkali. The latter is assumed to be dominated by excitation of the resonance line and by ionization. Under this condition, energy conservation reads

$$\begin{aligned}
 d/dt(3/2[e^-]Te) = & e[e^-]v_d \cdot X - [e^-][Xe]\sigma_{el}\left(\frac{2Te}{m_e}\right)^{1/2}\left(\frac{2m_e}{M_{Xe}}\right)(Te) \\
 & - [e^-][K]\left\{\overline{\epsilon_{res}f(\epsilon)v(\epsilon)\sigma_{res,K}} + \overline{\epsilon_{ioniz}f(\epsilon)v(\epsilon)\sigma_{ioniz,K}}\right\} \\
 = & 0 .
 \end{aligned}
 \tag{11}$$

where  $f(\epsilon)$  is the Maxwellian energy distribution and the bar indicates the appropriate integration over electron energy. For computations, we will, as a first approximation, set<sup>5</sup>

$$\overline{f(\epsilon)v(\epsilon)\sigma(\epsilon)} = \frac{6 \cdot 10^2}{(e/m_e)/\pi} \frac{d\sigma}{d\epsilon} \bigg|_{\epsilon_0} \left(\frac{2}{m_e} Te\right)^{3/2} \exp(-\epsilon_0/Te) \left(1 + \frac{\epsilon_0}{2Te}\right)$$

where  $\epsilon_0$  is the threshold energy for the excitation or ionization process. Here,

[ ] indicates species concentration

$m_e$  is the electron mass

$v_{e(\epsilon)}$  is the electron velocity =  $(2\epsilon/m_e)^{1/2}$

$\sigma_{el}$  is the elastic collision cross section of electrons with the xenon at an energy  $\approx Te$

$(2m_e/M_{Xe})$  is the fractional energy loss per elastic collision

Subscripts "res" and "ioniz" refer to the resonance and ionization level of the potassium

The drift velocity,

$$v_d = (2Te/m_e)^{1/2} \left( \frac{m_e}{M} \right)^{1/2}$$

$e$  is the electron charge

$X$  is the electric field in the plasma.

### 2. Electron Production

Electrons are produced through photoionization of the alkali by an external uv flux and by electron collisional ionization of the alkali and the rare gas. (In the uv sustainer mode photoionization will, of course, dominate.) Electrons are assumed to be lost through dissociative recombination. The steady state-rate equation for the electron density then reads

$$\begin{aligned} d/dt[e^-] = [K]\phi_{uv}\sigma_{PI} + [e^-][K]\overline{f_e v_e \sigma_{ioniz}} \\ + [e^-][Xe]\overline{f_e v_e \sigma_{ioniz, Xe}} - \alpha[e^-]^2 = 0, \end{aligned} \quad (12)$$

where  $\phi_{uv}$  is the effective ionizing photon flux,  $\alpha$  is an average dissociative recombination coefficient, and  $\sigma_{PI}$  is the photoionization cross section of the potassium.

### 3. Gas Temperature

Gas heating is primarily due to joule heating and occurs on a time scale that is short compared with that for thermal conduction. Therefore, the time-dependent energy equation is used with the specific heat due to the high pressure rare gas component:

$$d/dt(3/2[R. G.]Tg) = j \cdot E. \quad (13)$$

For computations we approximate  $j \cdot E$  and  $[R. G.]$  as constant and write:

$$T_g = T_o + \frac{(j \cdot E)t}{3/2[R. G.]} \quad (14)$$

where  $T_o$  is the oven temperature required for producing a specified equilibrium alkali vapor pressure.

Table II-2 lists some of the estimated values of the constants used in the plasma model. Clearly, the discharge pumping model is more approximate at its present state of development than is the optical pumping model because of the a priori use of Maxwellian energy distributions, truncated expressions for the electron collisional excitation and ionization rates, and uncertainties in the values of the electron collision cross sections. The model is expected to yield results correct to within an order of magnitude.

Examples of results for a self-sustained and uv-sustained discharge through K-Xe are shown in Figs. II-4 and II-5, respectively. The terms self-sustained and uv-sustained used here refer to situations where electron production in the plasma is dominated by electron collisional ionization or by uv photoionization, respectively. Whether or not a sustained discharge current can be made to flow under these conditions will depend on whether the current density is high enough to sustain electron emission into the discharge from the cathode. This current density threshold has not yet been determined. The results do illustrate, however, that practical laser gains on both the excimer and dimer bands in K-Xe can be achieved in either the uv or collisional ionization mode at a discharge power density far below the power densities which are now routinely used to excite atmospheric pressure  $CO_2$  laser mixtures using preionization conditioning of the discharge. The situation appears even more hopeful from the point of view of discharge stability since those mechanisms which are now believed to be most responsible for the glow-to-arc transition in the  $CO_2$  laser

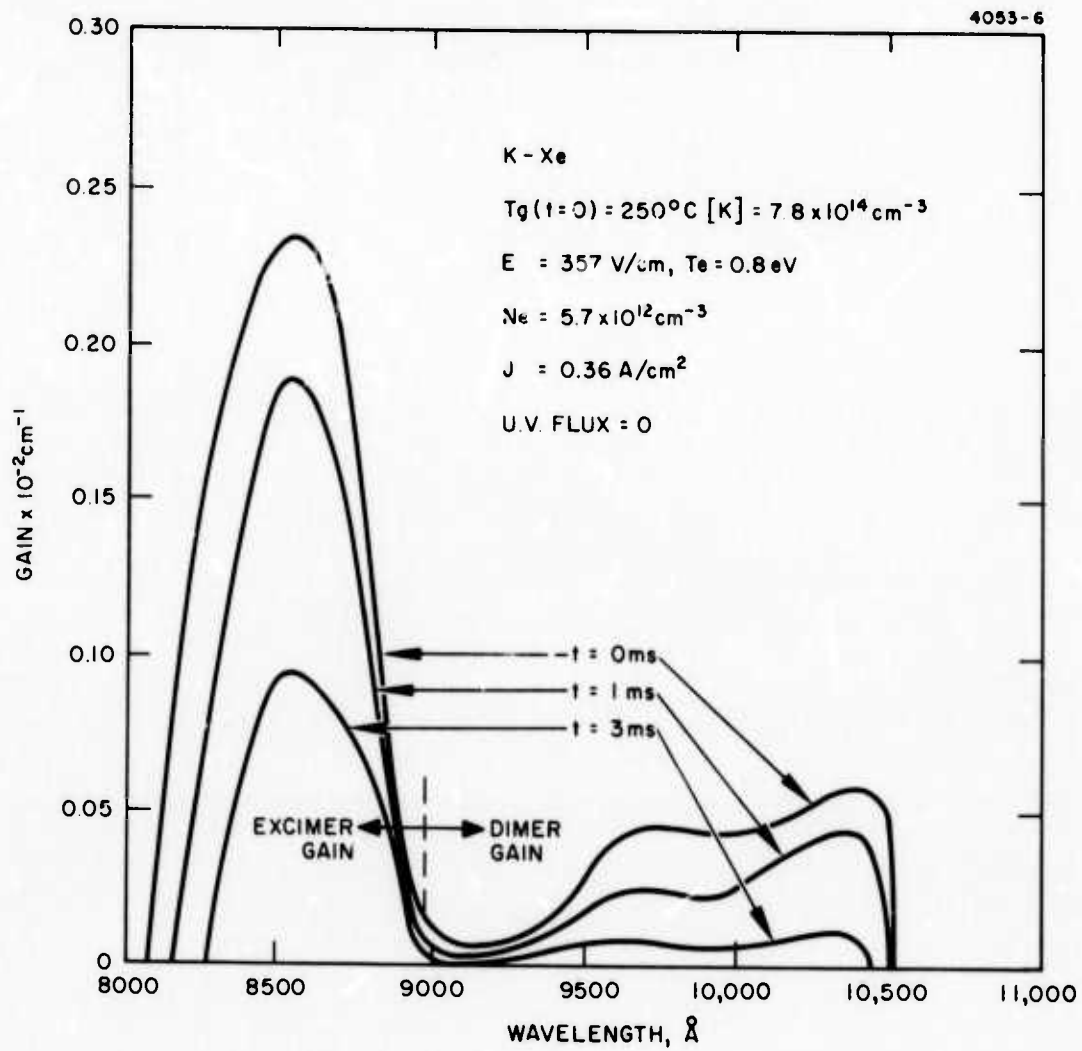


Fig. II-4. Potassium-xenon theoretical, small-signal laser gain - self-sustained discharge.

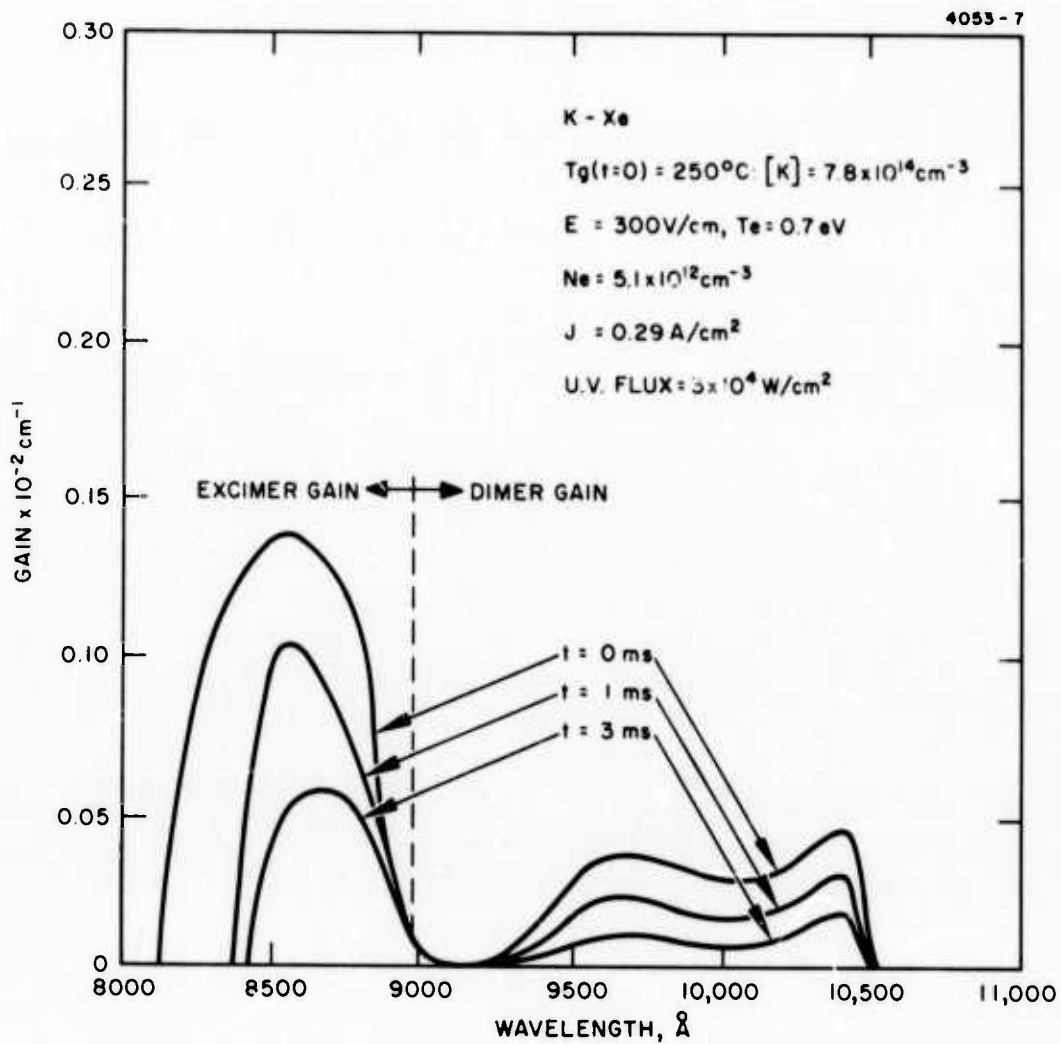


Fig. II-5. Potassium-xenon theoretical, small-signal laser gain — uv-sustained discharge.

Table II-2

## RATE CONSTANTS USED IN PLASMA MODEL

Cross Sectional Rate Constant	Estimated Value
$\sigma_{el}$	$3 \times 10^{-16} \text{ cm}^2$
$\sigma_{res, K}$	$1 \times 10^{-14} \text{ cm}^2$
$\sigma_{ioniz, K}$	$3 \times 10^{-16} \text{ cm}^2$
$\sigma_{PI, K}$	$1 \times 10^{-19} \text{ cm}^2$
$\alpha$	$3 \times 10^{-7} \text{ cm}^3 \text{ sec}^{-1}$

P1664

discharges (thermal deposition and attachment) will be present to a much lesser degree in an alkali-rare gas plasma. Other mechanisms peculiar to an alkali-rare gas mixture such as local cataphoresis effects may cause problems, however. This important aspect of the problem still needs careful study.

Also illustrated in the discharge results is the effect of discharge heating on laser kinetics. In the examples shown, the gain falls to less than half its initial value in times on the order of 3 msec due to gas heating. Thus, gas heating must be carefully controlled if cw or high pulse repetition rate operation is to be attempted.

### III. EXPERIMENTAL PROGRAM

Experimental studies of both a flashlamp pumped K-Xe system and, to a lesser degree, discharge pumped Cs-Ar and K-Ar systems have been carried out under the current program. The optically pumped experiments are, at present, being given highest priority in the attempt to demonstrate laser gain.

A versatile experimental apparatus employing a heated pressure vessel which is large enough to accommodate either the flashlamp pumped tube or a transverse discharge tube was used in the early phase of the program and is shown in Figs. III-1 and III-2, respectively. The re-entrant Brewster windows allow the vessel to be pressurized to several atmospheres.

Absorption coefficient measurements were initially made on both systems in order to verify the quasi-static model used in the computer calculations. A comparison, showing good agreement, between the measurements and the results of the theoretical model is shown in Figs. III-3 and III-4. Note the important contribution from the dimers, especially at the higher temperatures.

#### A. Discharge Experiments

One of the first electrode configurations chosen for the initial discharge studies is shown in Fig. III-5. This device employs uv pre-ionization of the discharge gap by a running spark discharge positioned below the anode screen as shown.

The first definitive observation of discharge-pumped excimer fluorescence was obtained with this device at a discharge current of  $\sim 3$  A flowing through a Cs-Ar mixture at  $\sim 5$  atm and  $250^\circ\text{C}$ . The waveforms of the preionizer spark current, the sustainer current, and the  $9000 \text{ \AA}$  Cs-Ar excimer emission from the discharge are shown in Fig. III-6. (The lower trace for the sustainer current and photomultiplier signal are for zero sustainer voltage.) The spectrographic

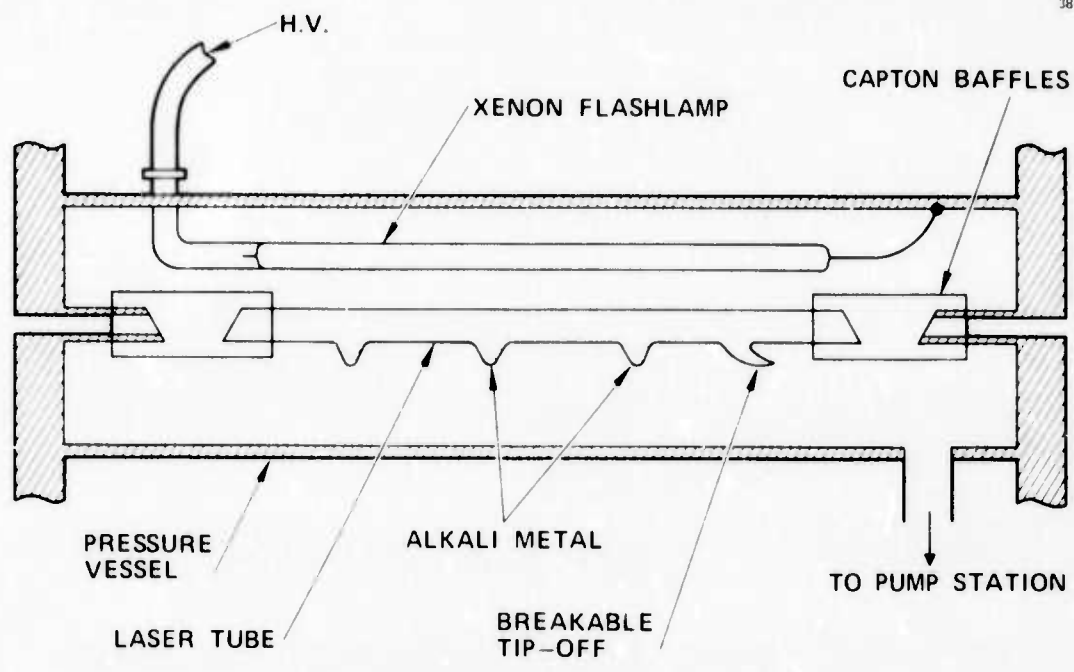


Fig. III-1. Old experimental apparatus - flashlamp pumping.

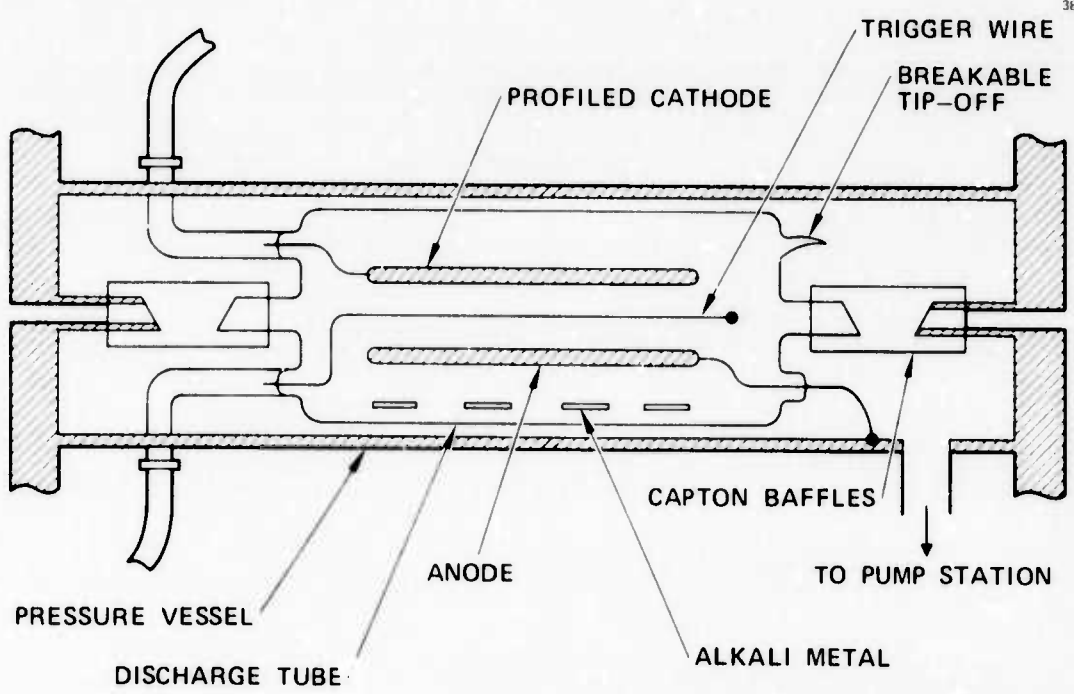


Fig. III-2. Old experimental apparatus - discharge pumping.

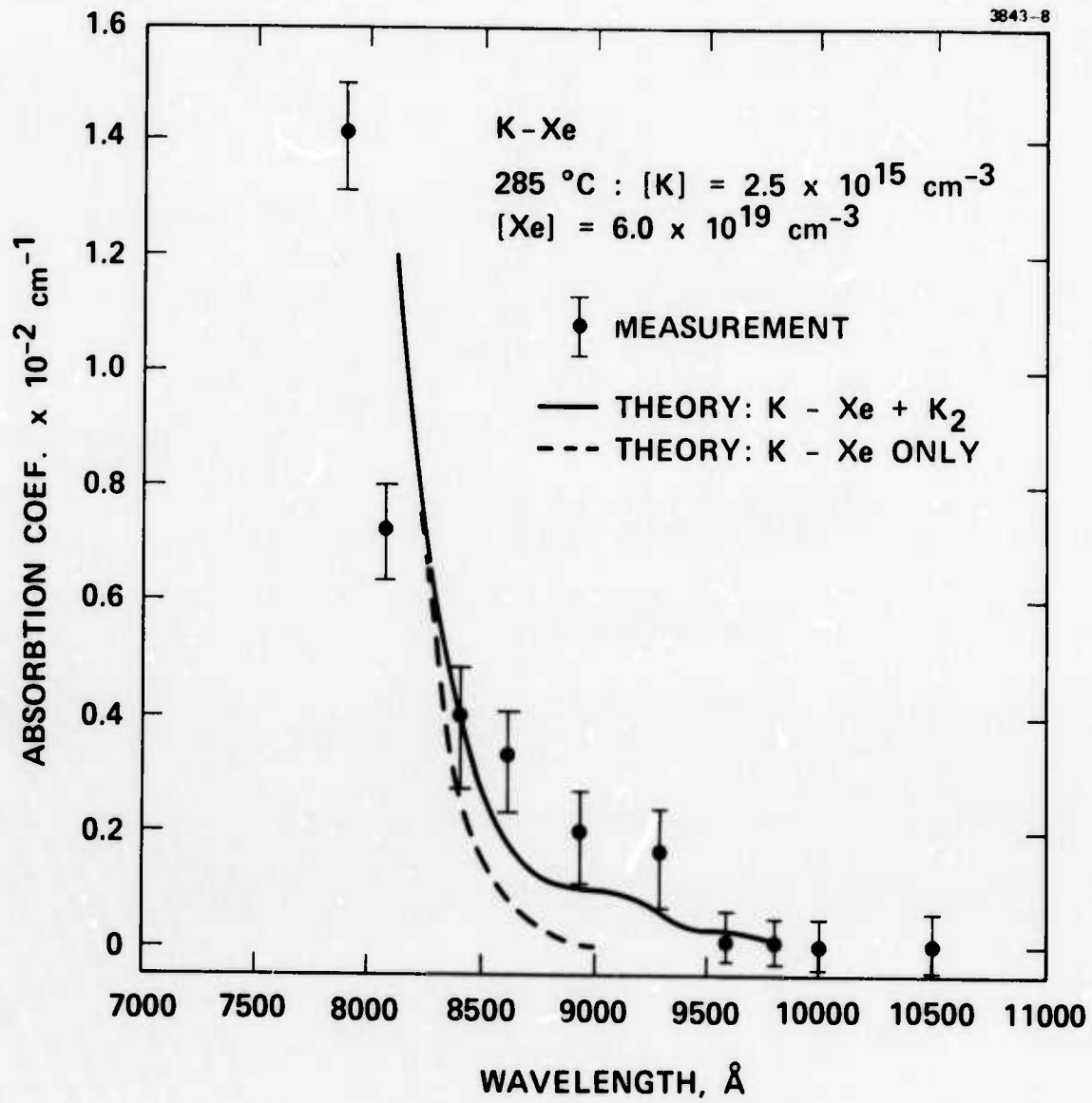


Fig. III-3. Potassium-xenon absorption coefficient: comparison of measurements with theoretical model (low temperature results).

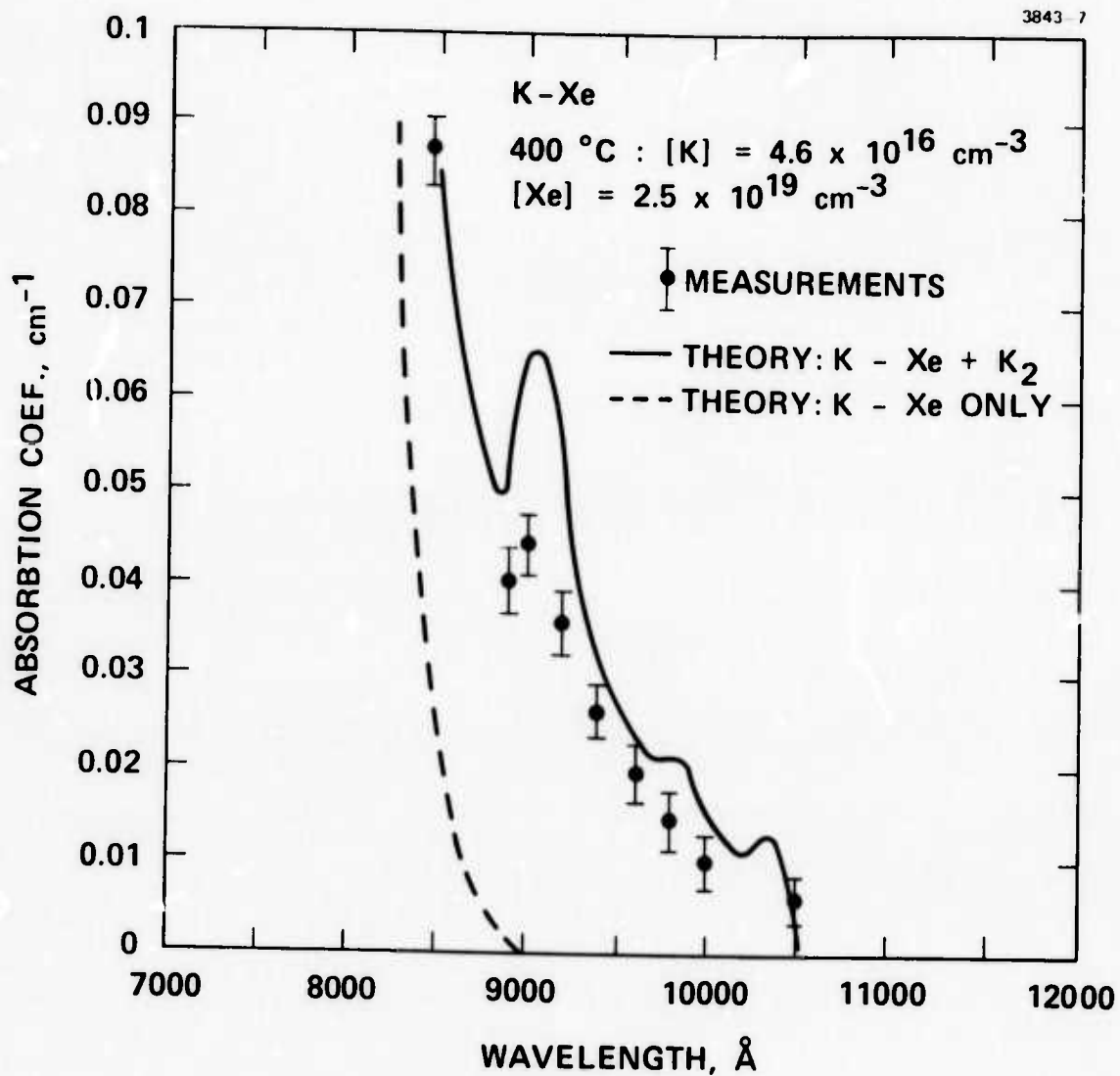


Fig. III-4. Potassium-xenon absorption coefficient: comparison of measurements with theoretical model (high temperature results).

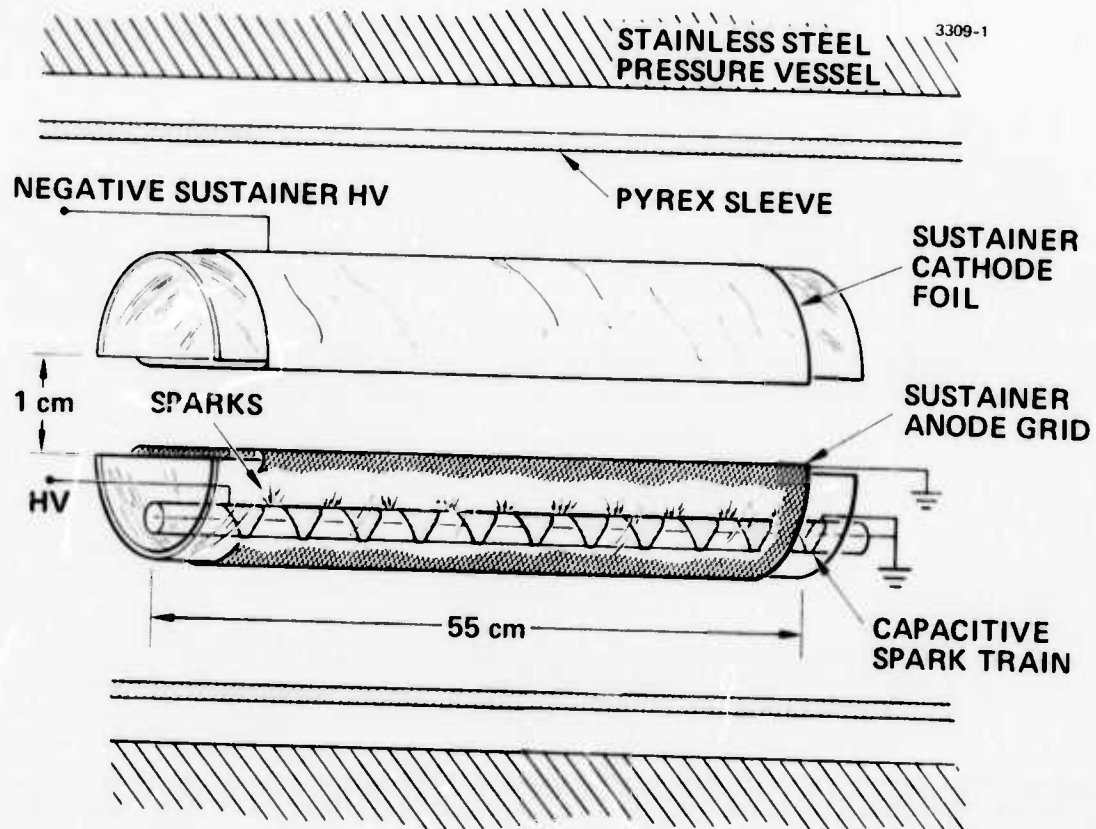


Fig. III-5. Present transverse discharge design.

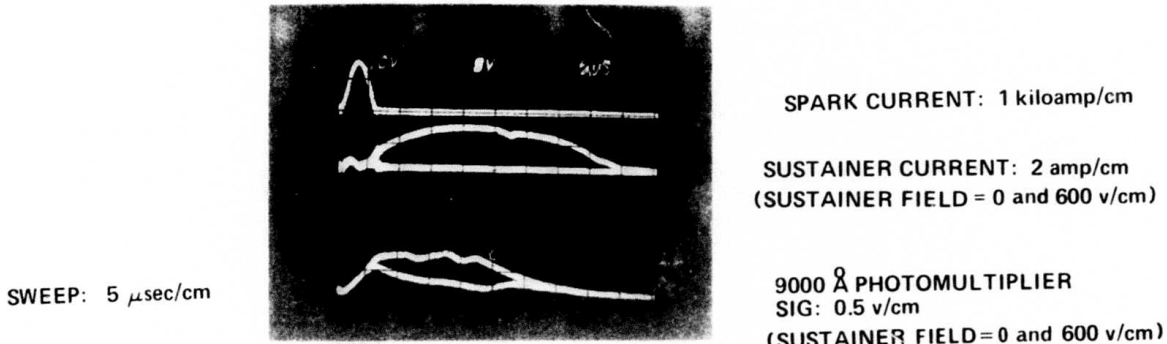


Fig. III-6. Current and excimer fluorescence waveforms.

profile of the emission was recorded on infrared-sensitive film and is shown in Fig. III-7. The continuum bands resulting from the  $A^2\pi_{3/2}$  to  $X^2\epsilon_{1/2}$  and  $A^2\pi_{1/2}$  to  $X^2\epsilon_{1/2}$  transitions are clearly visible as the red wings of the self-reversed 8521 Å and 8944 Å CsI resonance lines.

Photographs of the transverse profile of the discharge viewed from one of the end windows of the pressure vessel gave the appearance of a diffuse discharge. Assuming that this was the case, an estimate of the laser gain present on the  $A^2\pi_{1/2}$  to  $X^2\epsilon_{1/2}$  transition was made through a measurement of the spectral intensity of the fluorescence:

$$\text{Gain} = \frac{\lambda^4}{4\pi^2 c} P_\lambda \quad (\text{for large inversions})$$

$$P_\lambda \approx 2.10^{-3} \text{ watts}/(\text{cm}^3 \text{ \AA})$$

$$\text{Gain} \approx 3 \% \text{ per meter.}$$

This result was encouraging except for an increasing doubt as to whether the discharge was truly uniform throughout the length of the electrode gap. The photographs taken of the discharge inevitably defocus any longitudinal inhomogeneities. Also, reliable operation of the running spark along its entire length became very difficult as cesium was evolved into the mixture due to an arc shunting of the sparks to the screen. Thus it was doubtful that the main discharge gap was being illuminated and preionized uniformly along its entire length.

A new discharge tube was then constructed which employed the trigger wire double discharge technique to preionize the discharge. This is the discharge configuration shown in Fig. III-2. Here, again, it was not possible to reliably evaluate the spatial profile of the discharge because of the inability to view along the longitudinal dimension. It was doubtful that a uniform discharge was ever established under the

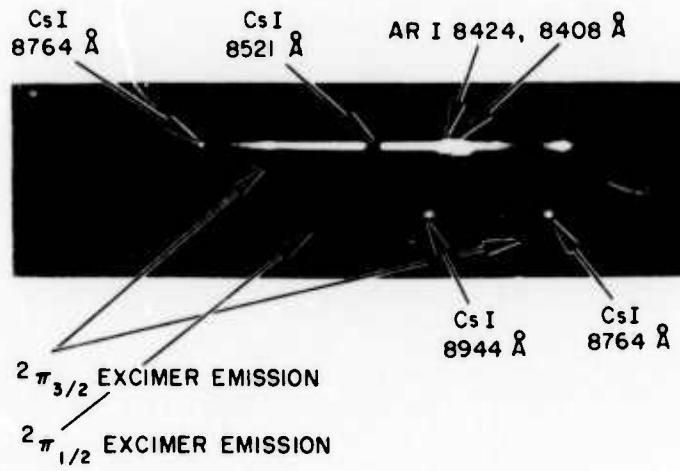


Fig. III-7. Excimer emission spectral profiles.

5 to 10 atm total pressure condition required for achieving a practical laser gain. It was possible, however, to establish a cw glow discharge through a K-Ar mixture at an argon concentration of  $\sim 4 \times 10^{17} \text{ cm}^{-3}$  at  $350^\circ\text{C}$ . The familiar deep red glow of the positive column and bluish emission of the negative glow adjacent to the cathode was readily observed under these conditions and the spectral profile of both the excimer and dimer bands was recorded. The relative profile of the observed emission was compared with the modeling results and showed excellent agreement, as shown in Fig. III-8.

At this point in the program it was decided to work exclusively with the flashlamp pumping technique for the remainder of the current program as the most expedient means to demonstrate gain. There can be no doubt that flashlamp pumping is uniform throughout the length of the mixture and the theoretical modeling for flashlamp pumping, which is far more accurate than the discharge modeling, predicts a large laser gain under easily attainable laboratory conditions.

#### B. Flashlamp Pumping Experiments

The initial flashlamp pumping experiments began with the use of the same pressure vessel that was used for the discharge experiments. The principal difficulty with this configuration was with the high voltage connection to the flashlamp which was within the heated region and, even more problematic, was immersed in a xenon gas environment which has a low breakdown threshold even at the high pressures used. The insulation provided for the connection would inevitably deteriorate at the high temperatures and arcing would occur from the connection to the pressure vessel causing breakage of both the tube and the flashlamp.

To remedy this problem and to generally upgrade and simplify the apparatus for flashlamp pumping, a new configuration was designed and fabricated which illuminates the need for the pressure vessel. The new configuration is illustrated schematically in Fig. III-9 and photographically in Fig. III-10. This heavy wall Pyrex laser tube has

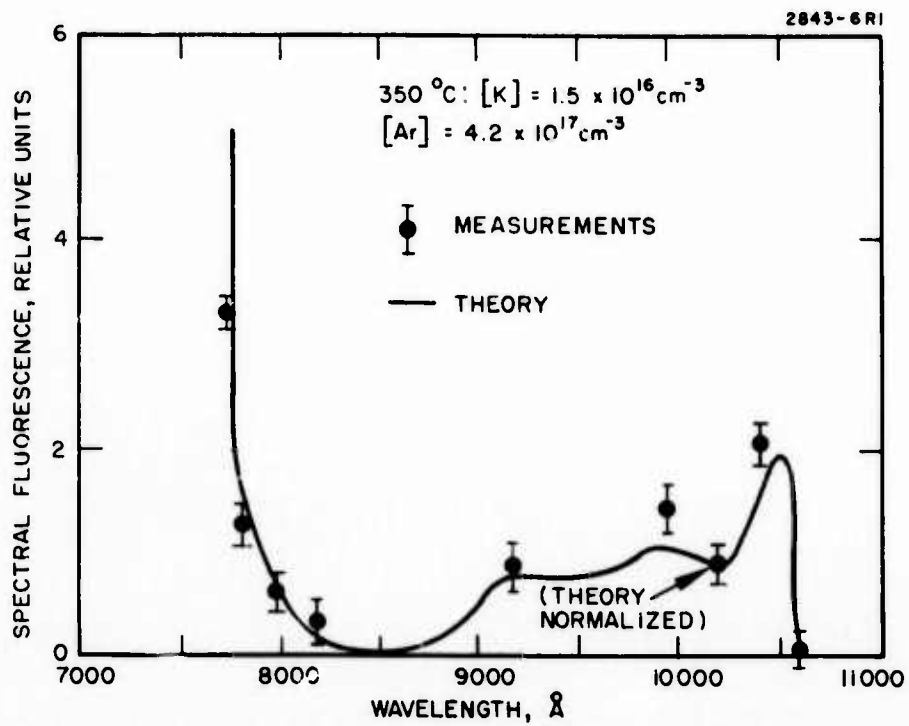


Fig. III-8. Potassium-argon discharge fluorescence comparison of measurements with theoretical model.

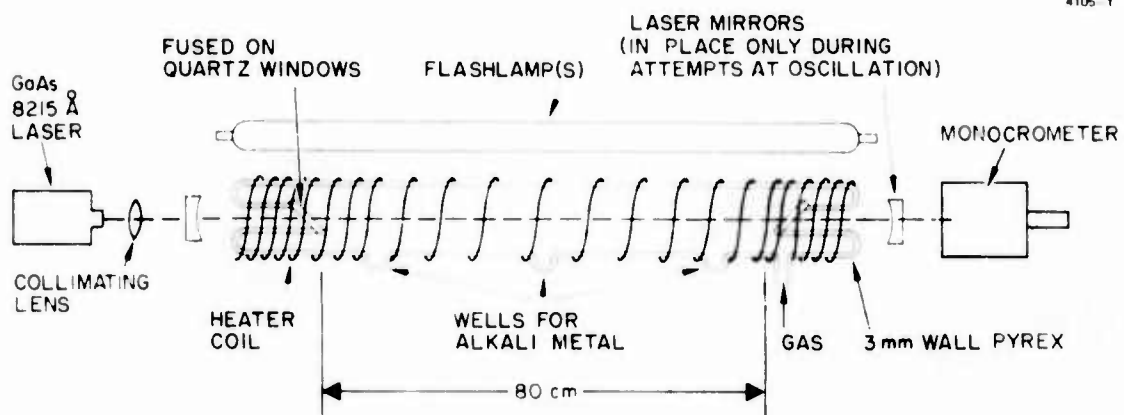


Fig. III-9. Current experimental apparatus.

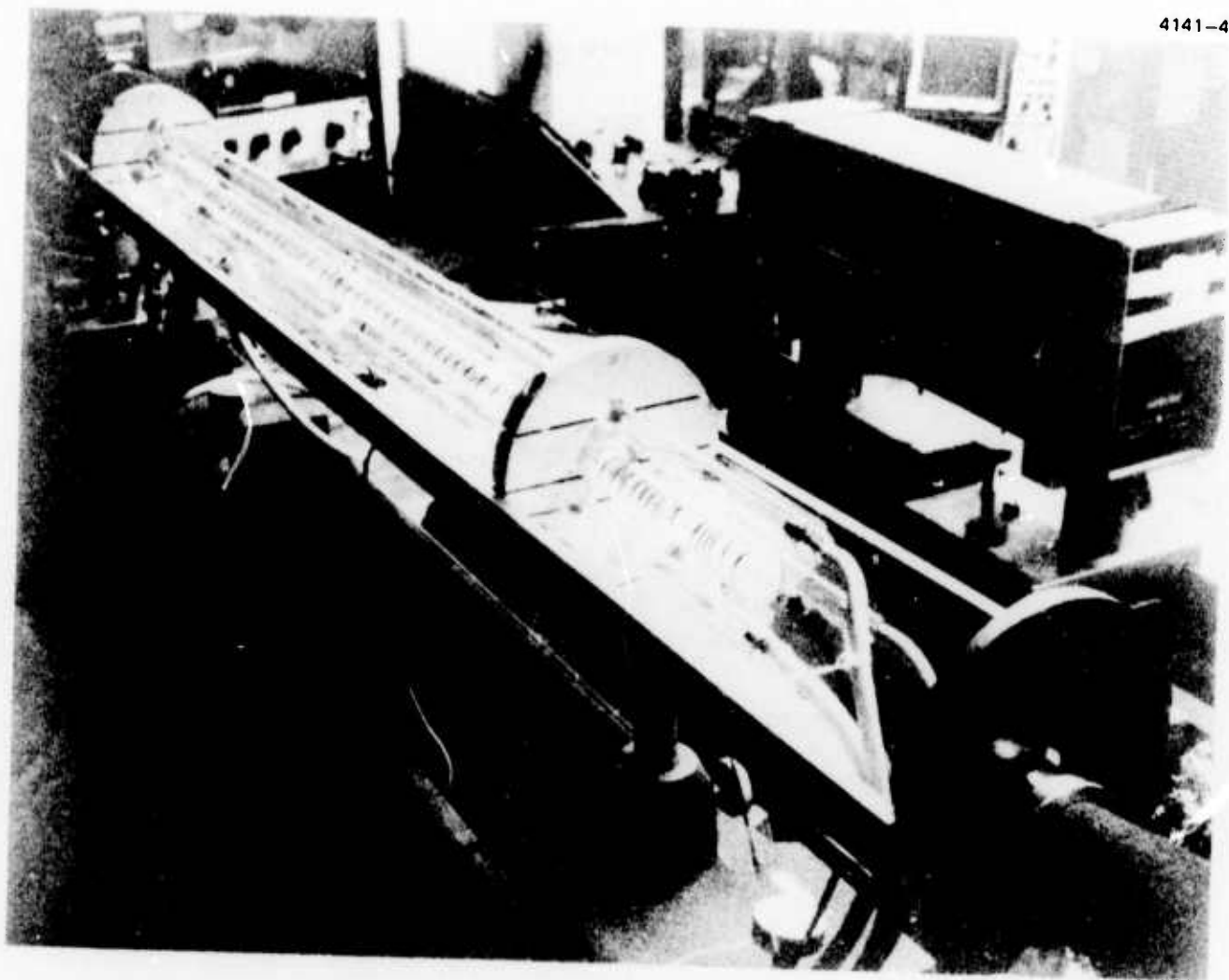


Fig. III-10. Photograph of present experimental apparatus.

operated reliably at total pressures of up to 20 atm and temperatures of up to 350°C without serious physical deterioration. The quartz Brewster windows are fused onto quartz stems which in turn are fused with graded seals onto the re-entrant Pyrex. Thus the tube is free of any adhesive which would degrade at the high temperatures employed in the experiments. The arcing problem is eliminated since the flashlamps are now in air and no longer in close proximity with a pressure vessel.

As indicated by Fig. III-9 this apparatus is being used both in attempts at achieving laser oscillation and for carrying out direct measurements of the laser gain through the use of a Ga-As probe laser. The system currently being studied is the K-Xe system. Fluorescence measurements are not possible with flashlamp pumping in the current setup due to the flooding of the monochromator with flashlamp radiation in the fluorescence bands which is scattered down the axis of the laser tube.

With the ability to view the longitudinal profile of the laser mixture in the new configuration, an important observation was made possible. As the tube walls are being heated, a potassium aerosol cloud is observed to be evolved into the mixture. After one to two hours after reaching a steady wall temperature, most of the aerosol cloud has dispersed but some aerosol always remains as evidenced by the forward scattering of a He-Ne laser beam passing through the mixture.

One attempt at achieving oscillation with one meter focal length mirrors coated for 99.9% reflection at 7600 to 8500 Å has been made on the current system with negative results. The scattering loss caused by residual aerosol present in the mixture during this attempt is regarded as a probable cause for the failure of oscillation.

The aerosol problem should be curable by various heating techniques which ensure that the xenon gas is maintained at a slightly higher temperature than the alkali metal. For the present, however, we have undertaken measurements of gain which can be carried out independent of the presence of cavity losses such as aerosols, window contamination, etc.

A 100 nsec Ga-As laser pulse is fired down the axis of the laser tube at a time corresponding to the peak of the flashlamp pumping, as in Fig. III-11, and again at a time outside the flashlamp pulse. The relative amplitude of these two Ga-As laser pulses as seen by the photomultiplier in Fig. III-9 is then a direct measure of the gain. The GaAs laser in use at present is at  $8215 \text{ \AA}$ . Thus it probes a region of the K-Xe excimer band which should exhibit about a 50% gain in passing through the 80 cm tube length (for the flashlamp flux assumed for the modeling results presented in Fig. II-2. The wavelength  $8215 \text{ \AA}$  lies outside the wavelength region for net gain, but this is immaterial for these measurements as long as the probe laser can penetrate through the length of the mixture.

In taking probe laser gain measurements through a 10 atm Xe-K mixture, it is important to monitor the possible refractive disturbance on the propagation of the probe beam due to thermal deposition into the mixture from the flashlamps. This is being done through the study of the propagation of a cw He-Ne laser beam through mixture during and subsequent to the flashlamp pulse. Acoustic disturbances on the beam propagation have been observed but the amplitude of these disturbances are only on the order of one percent and therefore should not interfere with the gain measurements. Also, a calibrated photodiode and a scanning multichannel spectrum analyzer have been used to obtain absolute measurements of the flashlamp spectral output power confirming that the flashlamp flux at the axis of the laser tube can be made at least as high as the flux value assumed in the modeling calculations (Fig. III-12).

The probe laser gain measurements are currently under way and data are presently being obtained which may indicate gain but are inconclusive at present pending a statistical analysis or a reduction of shot-to-shot fluctuations of the probe laser throughput to the photomultiplier caused by vibrations and convection currents in the high density gas.

4189-1

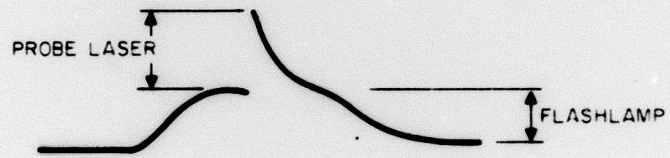
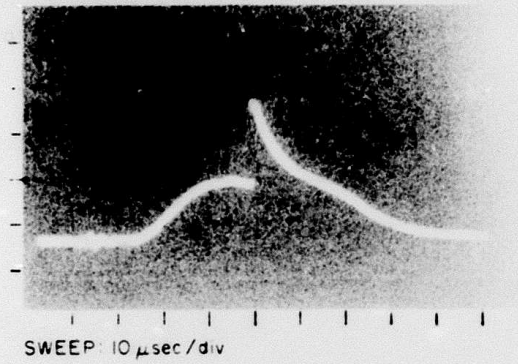


Fig. III-11. Probe laser gain measurement technique. Probe laser and flashlamp waveforms.

4141-5  
PRIMARY PUMP BAND: 7700 - 8100 Å

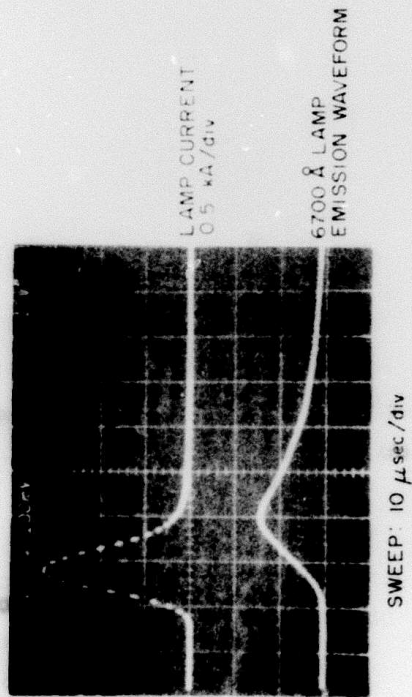
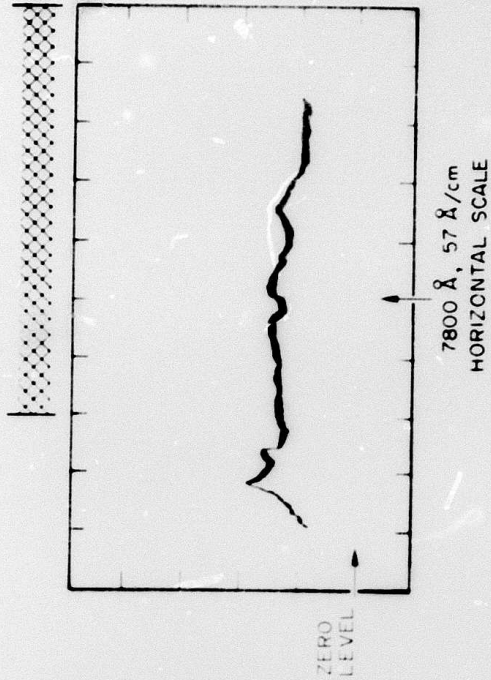


Fig. III-12. Flashlamp output measurements.

#### IV. FUTURE PROGRAM PLAN

##### A. Theoretical Modeling

By the end of the current program modeling predictions of the small signal gain versus wavelength and experimental parameters for all of the alkali-xenon A-X excimer and dimer transition will be completed for pumping by flashlamps, avalanche discharge, and uv sustainer discharge. Results will be presented in the form of Figs. II-2 through II-5, together with flow diagrams and listings of the computer codes.

##### B. Experimental Program

By the end of the current program the results of the probe laser gain measurements will be presented for at least two wavelengths within the K-Xe excimer band as a function of experimental parameters. Using the gain measurements as a guide, further attempts at oscillation within the excimer and dimer band of K-Xe will be carried out. Further measurements of the gain will then be made through the use of variable attenuators within the laser cavity.

##### C. Alkali Source Studies

By the end of the present program a survey will have been completed of alternative alkali vapor sources with the objective of identifying the most practical and efficient technique for evolving alkali vapors into a high pressure rare gas environment.

## REFERENCES

1. A. V. Phelps, JILA Report No. 110, University of Colorado, Boulder, Colorado, September 15, 1972.
2. York and Gallagher, JILA Report No. 114, University of Colorado, Boulder, Colorado, October 15, 1974.
3. R. E. M. Hedges, D. L. Drummond, and A. Gallagher, Phys. Rev. A 6, 1519 (1972).
4. J. Pascale and J. Vandeplanque, unpublished CEA Report, March 1974.
5. A. von Engel, Ionized Gases (Oxford Clarendon Press, 1965), Appendix 3.
6. O. S. Heavens, J. Opt. Soc. Am. 51, 1058 (1961).